THE ANNALS OF "DUNĂREA DE JOS" UNIVERSITY OF GALAȚI
FASCICLE V, TECHNOLOGIES IN MACHINE BUILDING,
ISSN 1221- 4566, 2012

FATIGUE LONG TERM DECK STRUCTURAL ASSESSMENT BASED ON DYNAMIC STRESS RESPONSE, OF A 100000 CBM LPG CARRIER

Iulia Mirciu,Ionica Rubanenco,Leonard Domnisoru

"Dunarea de Jos" University of Galati, Faculty of Naval Architecture, Romania
iuliamirciu@yahoo.com

ABSTRACT

The purpose of this work is to analyse the fatigue damage at the joint between the main deck structure and the transversal web frame (near x/L=0.6) composed of butt weld plate joints, in order to estimate the initial design ship service life period. The analysis adopts the hot spot approach based on three dimensional finite elements. The stress concentration factor is estimated using a linearization of the calculated longitudinal normal stress and equivalent von Mises stress around the hot spot. Fatigue damage is calculated by Palmgreen – Miner method for the initial ship hull structure, based on the long-term prediction ship dynamic response, using the cumulative damage ratio criterion, for the North Atlantic and World Wide Trade wave significant height histogram. The numerical analyses are carried out for a large double hull LPG Carrier with 230.4 m length between perpendiculars.

KEYWORDS: fatigue damage, life period, hot spot, stress concentration factor

1. INTRODUCTION

The present day ship design rules [9],[10] require the evaluation of the ship service life starting from the early design steps, based on the initial ship hull structural concept.

In this study, the numerical analyses are carried out on a double hull large LPG carrier, with elastic girder, considering the full and ballast conditions, under equivalent quasi-static head wave external load (1D-beam model and 3D-FEM model) and under extreme head irregular wave loads (hydroelasticity analysis). The main dimensions of a large liquefied petroleum gas carrier ship are presented in Section 2.

The ship structural requirements also impose to develop three-dimensional (3D) models, based on the FEM Finite Element Method ([8], [13]).

In Chapter 3 are presented the numerical results for 1D – girder, 3D – FEM global and 3D – FEM detail model for a LPG Carrier 100000 cbm.

In the standard seakeeping analyses, the wave induced ship dynamic response includes only the ship rigid hull oscillations ([1]). For large elastic ships, the wave induced ship dynamic response includes also oscillations (low frequency) and vibration (high frequency) components [5].

In Chapter 4 the liquefied petroleum gas carrier wave induced ship hull dynamic response is obtained, in the hypotheses of the hydroelasticity theory, including the following components: the linear and non-linear oscillation response, the springing phenomenon, linear and non-linear steady state vibration response, due to the ship structure-wave resonance, and the whipping phenomenon, bottom and side slamming induced transitory vibration response ([11], [4], [5], [15]).

In order to evaluate the design service life (Chapter 6) and the ship hull structure fatigue strength analysis based on Palmgreen –Miner cumulative damage ratio method ([9],[10],[14]) were used the steel standard S-N fatigue design curves and two long term wave significant height histograms: North Atlantic and World Wide Trade. Based on the fatigue analysis, an approximate initial prediction of the ship service life at the early design stage is obtained, considering a travel scenario with equal probabilities of the two loading cases. This topic is approached in Chapter 6.

The conclusions of this study are included in Chapter 7.

2. GENERAL SHIP DATA

In this study it is considered a large liquefied petroleum gas carrier ship LPG 100000 cbm, with double hull and

structural independent cargo tanks. The main dimensions of the ship are presented in Table 1.

Table 1. *The main dimension of LPG carrier*

Type of ship	LPG Carrier
Hull type	Mono-hull
Overall length, L_{OA}	238.7 m
Length between perpendiculars, L_{PP}	230.4 m
Length of water line at T, L_{WL}	227.2 m
Breadth moulded, B	38.2 m
Depth of main deck, H	23.2 m
Block coefficient, C_B	0.77
Maximum service speed	17 knots

According to the Bureau Veritas Rules [3], for the LPG 100000 cbm carrier are considered two main loading cases, presented in Table 2, with the following mass diagrams:
− in Fig. 1, the full cargo load case 1;
− in Fig. 2, the normal ballast load case 2.

Table 2. *The ship loading cases*

No	Case	d_m[m]	d_{aft}[m]	d_{fore}[m]
1	Full	12.32	11.32	13.43
2	Ballast	8.74	8.16	9.30

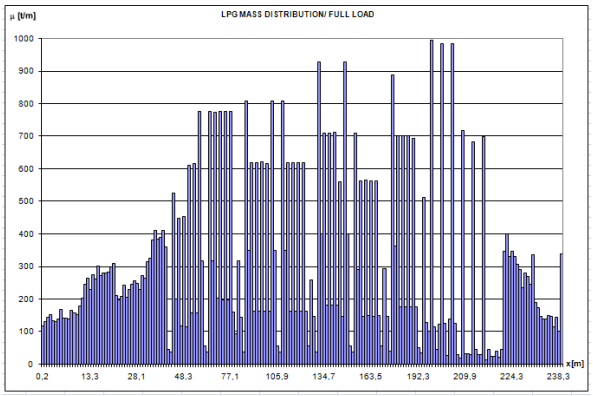

Fig. 1. *Mass distribution – Full cargo load case*

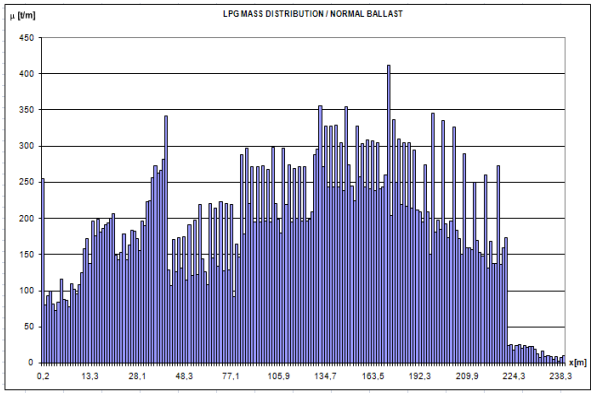

Fig. 2. *Mass distributions–Normal ballast case*

3. NUMERICAL RESULTS: 1D-GIRDER, 3D-FEM GLOBAL MODEL AND 3D-FEM LOCAL MODEL FOR LPG STRENGTH ANALYSIS

3.1. Numerical results on 1D-Girder model

Knowing the shipload condition, based on the mass diagram and the ship hydrostatic diagrams, there are calculated for the 1D-girder model, using an iterative method, the bending moments, the shearing forces and the still water and for different external quasi-static head wave pressure with height h_w =0–12 m, step δh_w = 1 m and h_w = 10.270 m (equivalent quasi-static statistical wave height from rules) the vertical in plane equilibrium conditions.

The numerical results for the stresses obtained at main deck are represented in Fig.3 and Fig.4 in hogging condition for both load cases: full load and normal ballast condition. It is selected only the hogging condition, because in the sagging condition the maximum stress values are smaller.

Table 3. *The maximum (max) stresses at section 0.6L*

Load case	σ_{x_D} [N/mm^2]	
	Hogging	Sagging
Full cargo	224.554	40.070
Ballast	159.742	62.346

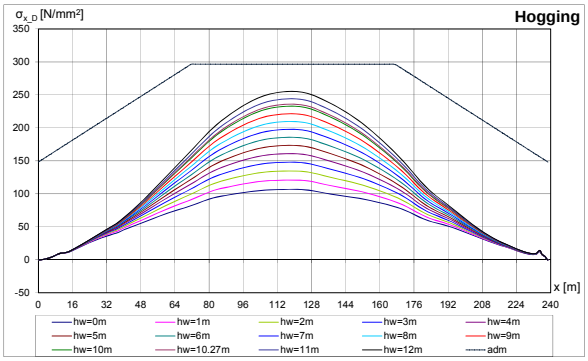

Fig. 3. *Maximum stresses at main deck on 1D-girder model, full cargo load*

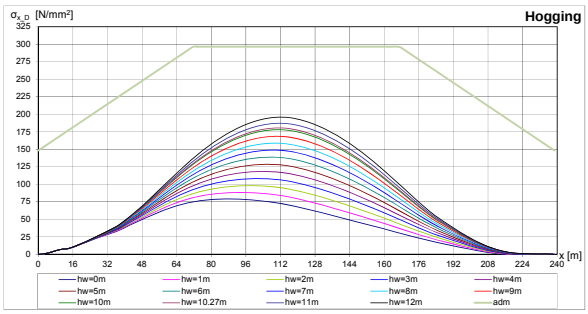

Fig. 4. *Maximum stresses at main deck on 1D-girder model, ballast load*

3.2. Numerical results on 3D-FEM global full extended model

The ship strength analysis includes the generation of the 3D-FEM hull model, based on the 3D-CAD model, with the auto-mesh options, that are usually included in the FEM programs. The average mesh size is one longitudinal standard space (about 800 mm), in all directions. For this model was necessary to use 171863 elements (plate, beam and rod), 448 element property and 2 material properties.

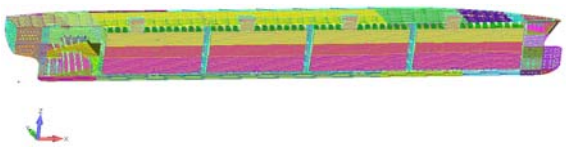

Fig.5. *3D-FEM LPG 100000 cbm ship model*

The boundary condition applied to the 3D – FEM model fully extended over the length are:

− the symmetry conditions at the nodes disposed in the centre plane of the ship, the model being developed only on one side;

− the vertical support conditions at two nodes disposed at the ship hull structure extremities (in the diametric plane), noted ND_{aft} at aft peak and ND_{fore} at fore peak.

At the vertical equilibrium conditions, at still water or equivalent quasi-static head wave cases, the reaction forces $RFZ(ND_{aft})$, $RFZ(ND_{fore})$ in the two vertical supports have to become zero.

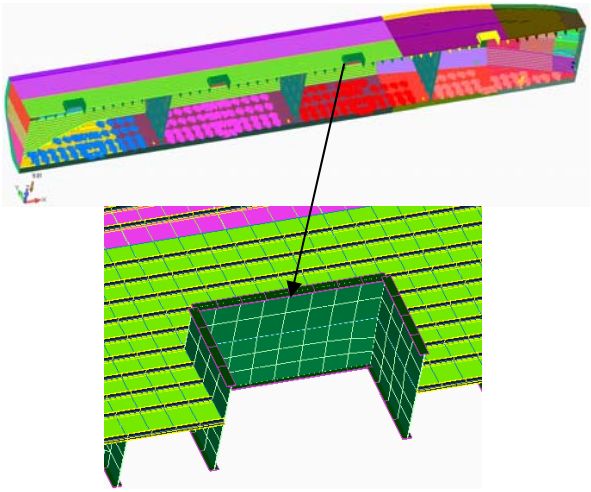

Fig. 6. *3D-FEM Cargo area structural details*

The loads acting over the ship hull structure are:

- the gravity load from the own hull structure weight and other mass components of the displacement, except the cargo;

- the cargo load, considered as local hydrostatic pressure over the cargo-holds structure;

- the equivalent quasi-static head wave pressure load for the following cases: h_w=0 (still water) and $h_w \neq 0$, according the statistical values from the Bureau Veritas Rules [3].

In the figures below, are represented only the numerical results for the stresses in hogging condition because in the sagging condition the maximum stress values are smaller.

In Table 4 are presented the numerical results in the equivalent quasi-static statistical wave height from rules (h_w = 10.270 m) for both load cases.

Table 4. *The maximum stresses at section 0.6L*

Load case	$\sigma_{von\ Mises\_D}$ [N/mm^2]		σ_{x_D} [N/mm^2]	
	$\sigma_{vonD\text{-}hog}$	$\sigma_{vonD\text{-}sag}$	$\sigma_{xD\text{-}hog}$	$\sigma_{xD\text{-}sag}$
Full	214.120	54.730	222.690	41.371
Ballast	152.570	65.542	155.100	67.443

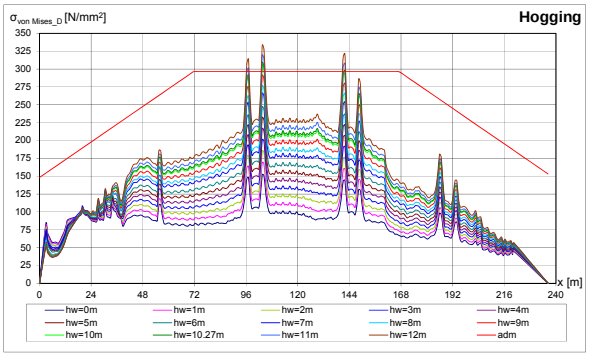

Fig. 7. *Maximum von Mises stresses at main deck, full cargo load*

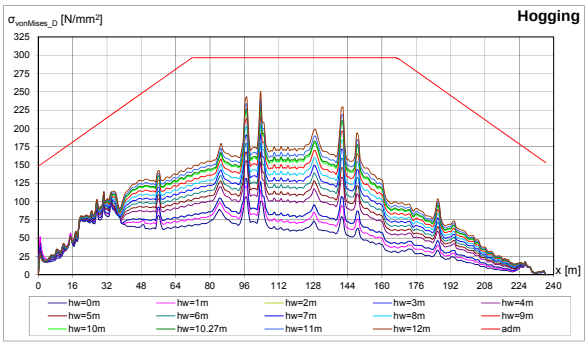

Fig. 8. *Maximum von Mises stresses at main deck, ballast load*

3.3. Numerical results on 3D-FEM detail local model

The maximum von Mises stresses are obtained (Fig.7 and Fig.8) near the dome and near to the transversal bulkheads.

In Fig. 6 is represented the 3D – FEM global model (structural mesh is about 800 mm) while in Fig. 9 is represented the 3D – FEM fine model meshing using approximately 25 mm (plate thickness). In the 3D–FEM global model are modelled only longitudinal structural elements of the holes and ducts without relief.

The transition from 3D–FEM global model to the 3D–FEM fatigue model (detail model) has been performed using automatic or manual modelling techniques, taking account the shape of the brackets, the flanges, etc. into the 3D–FEM detail model. All the constructive elements of the 3D–FEM detail model are modelled as plate elements.

For this model are necessary to use 1494422 elements (plate, beam and rod), 376 element properties and 2 material properties.

The purpose of this work is to analyse the fatigue damage at the joint between main deck structure and the transversal web frame (near to x/L=0.6) represented in Fig 10. The detail model has been implemented in the 3D–FEM global model.

The detail model is analysed using the same boundary condition and load cases but only for the equivalent quasi-static statistical wave height according to the rules (h_w = 10.270 m) [3],[9],[10].

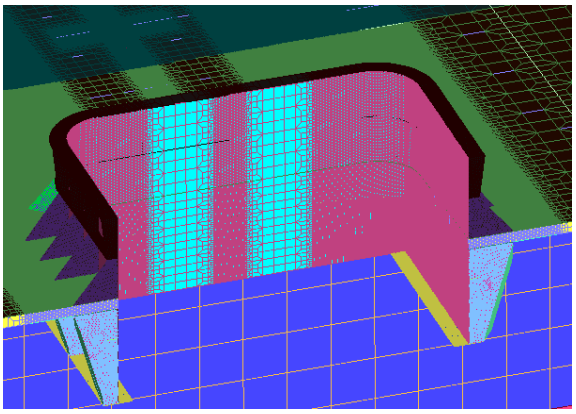

Fig. 9. *3D–FEM detail model, dome area*

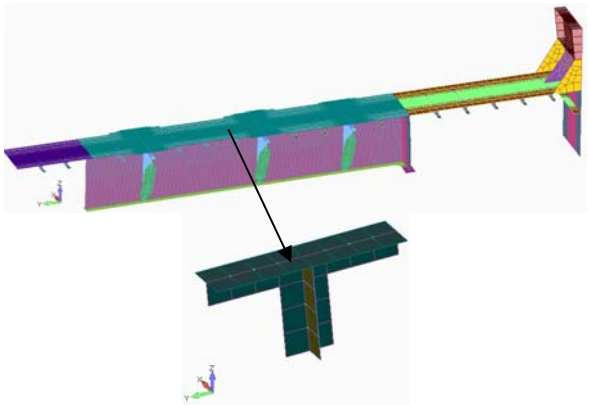

Fig. 10. *3D–FEM detail model, section near x/L=0.6*

In Table 5 are presented the numerical results for the equivalent quasi-static statistical wave height according to rules (h_w = 10.270 m) [3],[9],[10] in both load cases.

Table 5. *The maximum stresses at section 0.6L*

Load case	$\sigma_{von\ Mises\_D}$ [N/mm^2]		σ_{x_D} [N/mm^2]	
	$\sigma_{vonD\text{-}hog}$	$\sigma_{vonD\text{-}sag}$	$\sigma_{xD\text{-}hog}$	$\sigma_{xD\text{-}sag}$
Full load	242.330	38.270	202.470	32.724
Ballast	244.724	101.187	229.549	102.684

4. NUMERICAL RESULTS USING THE DYNAMIC ANALYSIS BASED ON THE HIDROELASTICITY THEORY

In this section, the analysis is focused on the linear and non-linear LPG Carrier 100000 cbm dynamic response in irregular head waves, based on the hydroelasticity theory.

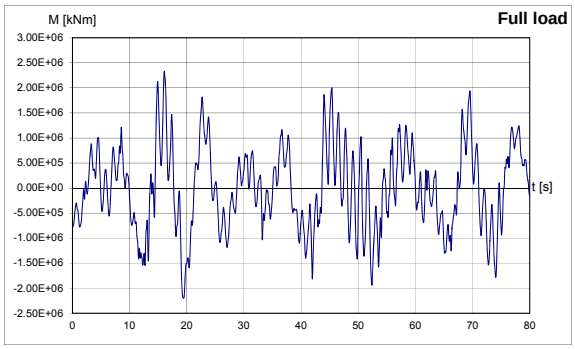

Fig. 11. *Non-linear analysis, time record, wave $h_{1/3}$= 10.270 m, bending moment amidships*

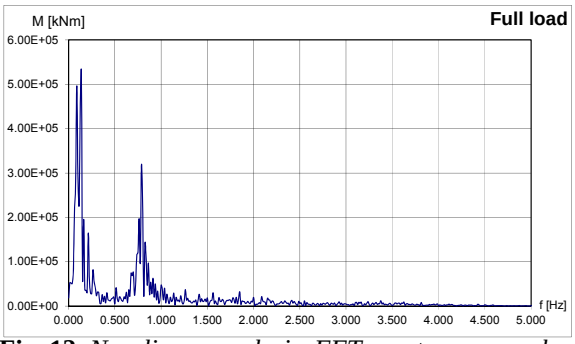

Fig. 12. *Non-linear analysis, FFT spectrum, wave $h_{1/3}$ = 10.270 m, bending moment amidships*

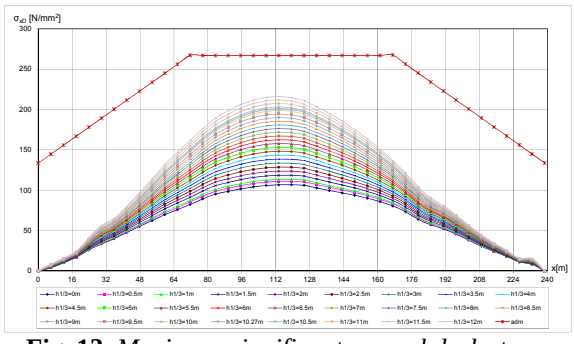

Fig. 13. *Maximum significant normal deck stress [N/mm^2], non-linear analysis + still water*

The theoretical model is based on the following hypotheses:

– the ship hull is modelled with 1D-FEM finite element method, using Timoshenko elastic beam finite element [2];

– the hydrodynamic excitation forces are modelled according to the hydroelasticity and strip theory, based on Gerristma and Beukelman model [1];

– the hydrodynamic coefficients are calculated based on the Porter & Vugts 2D potential fluid flow method [2];

– the ship dynamic response is decomposed, according to the modal analysis technique, on ship oscillation (low frequency, rigid hull) and vibration (high frequency, dry elastic hull) modes ([5],[6]);

– the excitation is the external head wave, model Longuet-Higgins ([5], [15]).

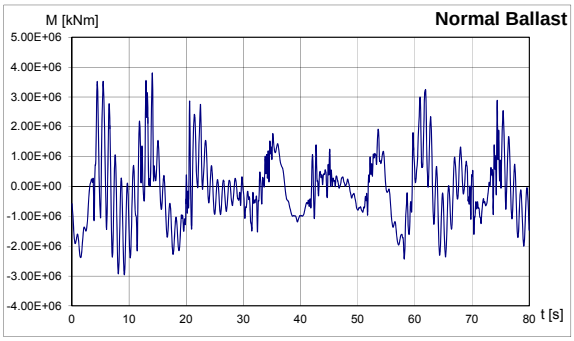

Fig. 14. *Non-linear analysis, time record, wave $h_{1/3}$= 10.270 m, bending moment amidships*

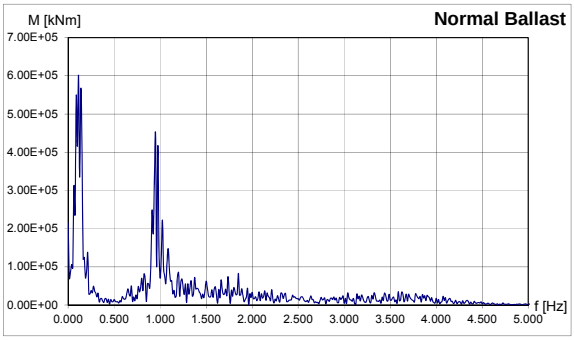

Fig. 15. *Non-linear analysis, FFT spectrum, wave $h_{1/3}$ = 10.270 m, bending moment amidships*

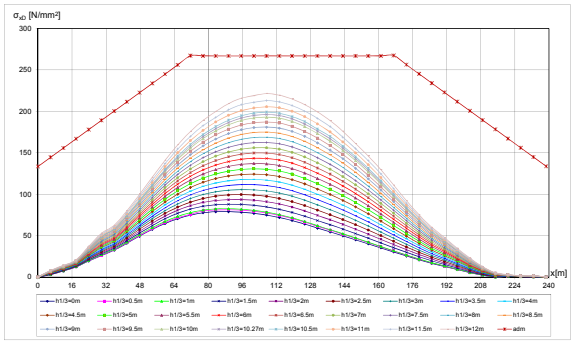

Fig. 16. *Maximum significant normal deck stress [N/mm^2], non-linear analysis + still water*

Because the excitation force includes the unknown non-linear dynamic response, it is necessary to use an iterative algorithm for the time domain solution of non-linear motion equations [5].

– the solution of the differential non-linear motion equations system, using a time domain integration procedure, β-Newmark, at each iteration, with simulation time T_s = 80 s and time step δt =0.01 s;

– the ship non-linear dynamic response;

– the spectral analysis of the total ship dynamic response with the Fast Fourier Transformation (FFT), short-term statistical parameters.

The dynamic analyses are carried out for the head waves first order spectra ITTC [1] with the significant wave height $h_{1/3}$ = 0–12 m, step $\delta h_{1/3}$ = 0.5 m, according to the Beaufort scale B_{level} = 0–11.

The numerical results for the hydroelastic response are synthesized in:

- In Fig. 11 and Fig. 14 is represented the bending moment time record, in Fig.12 and Fig. 15 is represented the bending moment amplitude spectrum FFT, for full load and normal ballast condition for the ship speed u_s =17 knots;
- In Fig. 13 and Fig. 16 is represented the maximum significant normal deck stress [N/mm^2], non-linear analysis +still water, $h_{1/3}$ = 0 − 12 m, u_s = 17 knots, full load and normal ballast condition.

5. HOT SPOT STRESS ANALYSIS

Such models may be used for the strength analysis of secondary or special structural components as well as stochastic fatigue analysis of structural details. Moreover, stress concentration models are used for the simplified fatigue analysis where the stress concentration is unknown [3], [9].

The stress concentration factors analysed here are defined based on the hotspot stress assessment of the welded connection between the main deck and the transversal web frame near x/L = 0.600.

The analysed hot spots are located on both sides of the weld (Fig. 17). The structures are subjected to uniformly distributed unit tensile stresses.

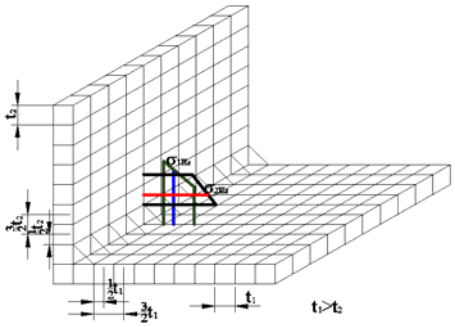

Fig. 17. *Hot spot stress definition*

Based on $\sigma_{hs} = 1.5\sigma_{0,5t} - 0.5\sigma_{1,5t}$, a linear stress extrapolation is performed for the x normal stresses and von Mises stresses, as indicated in Fig. 17, for the HS_1 and for the HS_2 respectively, using the same procedure. The hot spot stresses and stress concentration factors are estimated at the point of the maximum x normal stresses and equivalent von Mises stresses at the weld toe line.

From Tables 3, 4 and 5 it results that is the transposition coefficient from model 3D – FEM global model to 1D – girder model and from 3D –

FEM detail model to 1D – girder model are presented in Table 6. The transposition coefficients are the same with stress concentration factor.

Table 6. *The transposition coefficient for the calculated model*

x/L =0.6	Model 3D/1D – FEM global	Model 3D/1D – FEM detail
Full	1.366	1.079
Ballast	1.082	1.647

6. FATIGUE DAMAGE ANALYSIS

This chapter is focused on the initial service life evaluation for the LPG Carrier 100000 cbm, based on the fatigue strength assessment of the ship hull structure, using the maximum stresses for extreme wave loads obtained in the deck shell (Chapters 3–5).

To evaluate the ship fatigue strength criterion, with the Ship Classification Society Methodology ([9] and [10]), the cumulative damage ratio D method, based on Palmgren-Miner method and steel standard design S-N curves, is applied.

The cumulative damage ratio D has the following expression:

$$D_j = \sum_{i=1}^{m} \frac{n_i}{N_{i\_j,k}} \le 1 \qquad (1)$$

$$n_i = p_i \cdot n_{max\_j,k} \qquad N_{i\_j,k} = f_{SN}\left(\Delta\sigma_{ci}\right)$$

coupled with the histogram of the significant wave height for the selected navigation domain – North Atlantic scatter diagram and World Wide Trade;

n_i - the number of the cycles applied to the naval structure for the sea state $h_{1/3i}$;

N_i - the number of cycles from the fatigue strengths condition, based on the S-N diagram for $\Delta\sigma_{ci}$, corresponding to the sea state $h_{1/3i}$;

j represented the dynamic response in frequency domain and can be applied to the ship rigid body (oscillations) and also to the ship elastic hull (oscillations and vibrations);

k represented the global ship hull strengths, respective the wave loads for each load case.

The estimation of the exploitation life of the ship hull from the fatigue strengths criterion, based on the calculations made for R = 25 years, results from the following relation:

$$L = \frac{25}{D} \qquad (2)$$

$$D = 50\% \cdot D_{Full} + 50\% \cdot D_{Ballast}$$

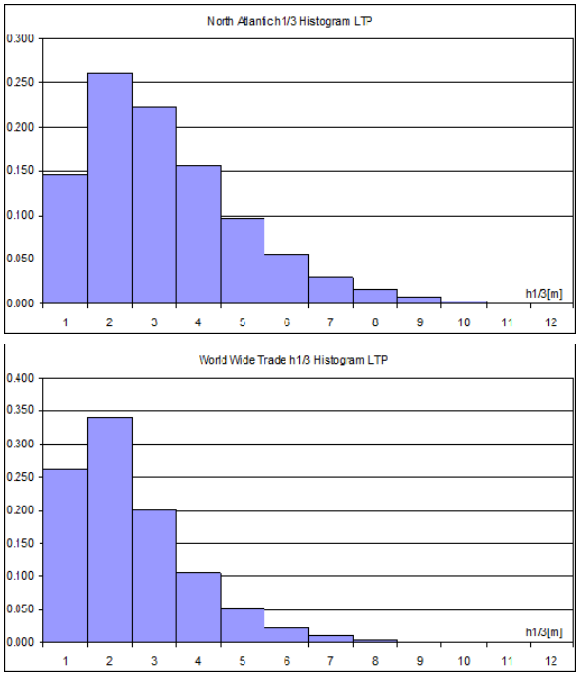

Fig. 18. *The histogram of the significant wave height $h_{1/3}$ on long-term period analysis*

The dynamic structural response induced from sea waves is obtained with the following methods:

- the determinist method based on the ship girder loads from the equivalent quasi-static wave.
- the spectral method, that requires a solution of the ship hull dynamic response in the frequency domain and can be applied to the ship rigid body (oscillations) and also to the ship elastic hull (oscillations and vibrations), but under linear hypothesis of the excitation forces and of the motion equations.

This method is used for the standard seakeeping analysis (ADV) at linear ship hull oscillations, and also for the linear analysis in the hypothesis of the hydroelasticity theory (HEL and DYN-LN).

- the time domain analysis method of the stress field distribution, that makes possible to include the non-linearities from the ship-wave dynamic system, being completed with a spectral analysis based on the Fourier FFT method.

This method is based on the nonlinear model for the calculation of the ship hull dynamic response, in the hydroelasticity theory hypothesis (DYN-NLN).

The influence of the butt weld joints welding quality ([9] and [10]), standard or very good welding, is also taken into account for the initial ship service life evaluation.

In Table 7, Table 8 and Fig. 19 are presented the values of fatigue damage and estimated ship service life for the ship rigid body (oscillations) using the North Atlantic scatter diagram and in Table 11, Table 12 and Fig. 21, the same values for World Wide Trade scatter diagram.

In Table 9, Table 10 and Fig. 20 are presented the values of fatigue damage and estimated ship

service life for the ship elastic hull (oscillations and vibrations) using the North Atlantic scatter diagram. The Table 13, Table 14 and Fig. 22 – the same values for World Wide Trade scatter diagram.

Table 7. *Fatigue damage for the ship rigid body North Atlantic scatter diagram*

Model/ Analysis	1D	Global	Fine
	D_SN	D_SN	D_SN
ADV	0.120	0.130	0.148
HEL	0.470	1.099	2.699
DYN-LN	1.321	0.951	2.490
DYN-NLN	0.519	1.258	2.786
DYN-NLNB	0.146	0.404	1.086

Table 8. *Estimated ship service life (rigid body) North Atlantic scatter diagram*

Model/ Analysis	1D	Global	Fine
	L [years]	L [years]	L [years]
ADV	>25	>25	>25
HEL	>25	**22.757**	**9.263**
DYN-LN	**18.929**	>25	**10.042**
DYN-NLN	>25	**19.873**	**8.973**
DYN-NLNB	>25	>25	**23.029**

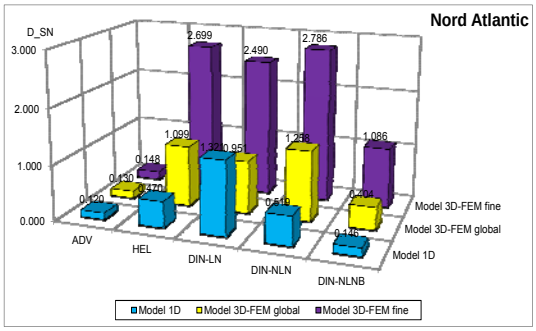

Fig. 19. *The fatigue damage for ship rigid body North Atlantic scatter diagram*

Table 11. *Fatigue damage for the ship rigid body World Wide Trade scatter diagram*

Model/ Analysis	1D	Global	Fine
	D_SN	D_SN	D_SN
ADV	0.039	0.043	0.048
HEL	0.159	0.381	1.028
DYN-LN	0.139	0.329	0.953
DYN-NLN	0.176	0.449	1.063
DYN-NLNB	0.049	0.136	0.392

Table 12. *Estimated ship service life (rigid body) World Wide Trade scatter diagram*

Model/ Analysis	1D	Global	Fine
	L [years]	L [years]	L [years]
ADV	>25	>25	>25
HEL	>25	>25	**24.321**
DYN-LN	>25	>25	>25
DYN-NLN	>25	>25	**23.521**
DYN-NLNB	>25	>25	>25

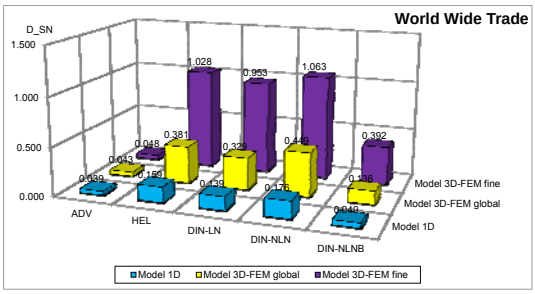

Fig. 20. *The fatigue damage for ship rigid body World Wide Trade scatter diagram*

Table 9. *Fatigue damage for the ship elastic hull North Atlantic scatter diagram*

Model/ Analysis	1D	Global	Fine
	D_SN	D_SN	D_SN
ADV	0.120	0.130	0.148
HEL	0.470	1.099	2.699
DYN-LN	1.321	0.951	2.490
DYN-NLN	0.747	1.743	4.963
DYN-NLNB	0.208	0.537	1.769

Table 10. *Estimated ship service life (elastic hull) North Atlantic scatter diagram*

Model/ Analysis	1D	Global	Fine
	L [years]	L [years]	L [years]
ADV	>25	>25	>25
HEL	>25	**22.757**	**9.263**
DYN-LN	**18.929**	>25	**10.042**
DYN-NLN	>25	**14.340**	**5.037**
DYN-NLNB	>25	>25	**14.129**

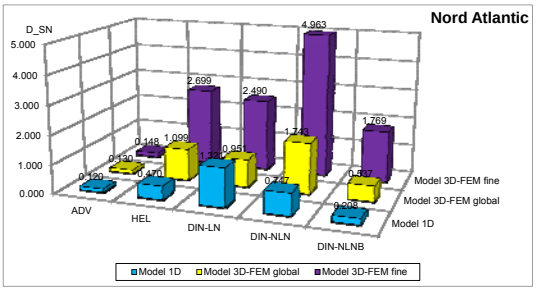

Fig. 21. *The fatigue damage for ship elastic hull North Atlantic scatter diagram*

Table 13. *Fatigue damage for the ship elastic hull World Wide Trade scatter diagram*

Model/ Analysis	1D	Global	Fine
	D_SN	D_SN	D_SN
ADV	0.039	0.043	0.048
HEL	0.159	0.381	1.028
DYN-LN	0.139	0.329	0.953
DYN-NLN	0.245	0.605	1.781
DYN-NLNB	0.067	0.179	0.603

Table 14. *Estimated ship service life (elastic hull) World Wide Trade scatter diagram*

Model/ Analysis	1D	Global	Fine
	L [years]	L [years]	L [years]
ADV	>25	>25	>25
HEL	>25	>25	**24.321**
DYN-LN	>25	>25	>25
DYN-NLN	>25	>25	**14.041**
DYN-NLNB	>25	>25	>25

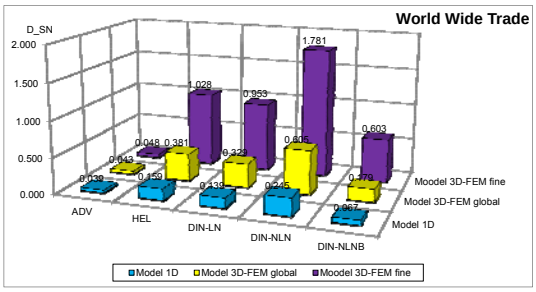

Fig. 22. *The fatigue damage for ship elastic hull World Wide Trade scatter diagram*

7. CONCLUSIONS

Based on the numerical results from Chapters 3–6, for the LPG carrier 100000 cbm hull structure (Chapter 2), it results the following conclusions:

1. The numerical results of the maximum values of normal stresses and equivalent von Mises stresses using the ship strength analysis, with quasi-static head wave are represented in Tables 3, 4 and 5, for each model at section 0.6L, pointing out the hot-spot resulting stresses.

2. The numerical results from the dynamic hydroelastic analysis indicate that the maximum stresses are recorded in the deck shell near at 0.6L.

3. The fatigue criterion based on the cumulative damage ratio method at extreme wave loads, for North Atlantic and World Wide Trade wave significant height histogram (Fig. 20), is analysed taking as reference the significant normal deck shell stresses.

In the case of ship rigid body (oscillations) the fatigue damage factor is:

- D_{SN} = 0.120 – 2.786 presented in Table 7, Table 8 and graphically in Fig.20, for North Atlantic wave significant height histogram;
- D_{SN} = 0.039 – 1.063 presented in Table 11, Table 12 and graphically in Fig. 22 for World Wide Trade wave significant height histogram.

In the case of ship elastic hull (oscillations and vibrations) the fatigue damage factor is:

- D_{SN} = 0.120 – 4.963 the values are presented in Table 9, Table 10 and graphic in Fig. 21 for North Atlantic wave significant height histogram;
- D_{SN} = 0.039 – 1.781 the values are presented in Table 13, Table 14 and graphically in Fig. 23 for World Wide Trade wave significant height histogram.

3. The values of fatigue damage based ship structure safety life evaluation in North Atlantic condition are smaller than the ones obtained using the World Wide Trade condition, because the North Atlantic is considered to be the one of the worst areas with respect to the extreme wave loads, so that the fatigue cracks in hull structure may appear earlier than other navigation conditions.

Acknowledgements

This study has been accomplished in the frame of the national grants EFICIENT POSDRU 88/1.5/S ID-61445 2009-2011 and TOP ACADEMIC POSDRU 107/1.5/S ID-76822 2010-2011.

REFERENCES

[1] **Bertram, V**., *Practical ship hydrodynamics*. 2000, Oxford, Butterworth Heinemann;

[2] **Bishop, R.E.D., Price,W.G**., *Hydroelasticity of ships*, 1979, Cambridge: University Press Cambridge;

[3] **BV**. 2006. Bureau Veritas Rules. Paris;

[4] **Domnisoru, L.**, Domnisoru, D., *The unified analysis of springing and whipping phenomena*, 1998, Transactions of the Royal Institution of Naval Architects London 140 (A), pp. 19–36;

[5] **Domnisoru, L.**, *Structural analysis and hydroelasticity of ships* [Book], 2006. Galati: University ''Lower Danube'' Press;

[6] **Domnisoru, L., Ioan, A**., *Non-linear hydroelastic response analysis in head waves, for a large bulk carrier ship hull*, Advancements in Marine Structures, Taylor & Francis Group, London, 2007, pp. 147–158;

[7] **Fricke W, Paetzold H. Full,** *Scale fatigue tests of ship structures to validate the S-N approaches for fatigue strength assessment,* Mar Struct 2010; 23(1), pp. 115–130;

[8] **Frieze, P.A., Shenoi, R.A**., *Proceeding of the 16*th *international ship and offshore structures congress (ISSC). Volumes 1 and 2*, 2006, University of Southampton;

[9] **GL**., *Guidelines for fatigue strength analyses of ship structures*. 2011, Hamburg: Germanischer Lloyd;

[10] **GL**, Germanischer Lloyd's Rules. 2011, Hamburg;

[11] **Guedes Soares, C**., *Special issue on loads on marine structures,* 1999, *Marine Structures,* 12(3), pp. 129–209;

[12] **Hughes, O.F**., *Ship structural design. A rationally based, computer-aided optimization approach*. New Jersey, 1988, The Society of Naval Architects and Marine Engineering;

[13] **Jang, C.D., Hong, S.Y.,** *Proceeding of the 17th international ship and offshore structures congress (ISSC). Volumes 1 and 2*, 2009, Seoul National University;

[14] **Mansour, A., Liu, D.,** *Strength of ships and ocean structures*. 2008, New Jersey: The Society of Naval Architects and Marine Engineering;

[15] **Perunovic, J.V., Jensen, J.J.,** *Non-linear springing excitation due to a bidirectional wave field*, Marine Structures 18, 2005 pag 332–358;

[16] **Rozbicki, M., Das, K., Crow, A**, *The preliminary finite element modelling of a full ship*, 2001, International Shipbuilding Progress Delft 48 (2), pp. 213–225;

[17] **Servis, D., Voudouris, G., Samuelides, M., Papanikolaou, A**., *Finite element modelling and strength analysis of hold no.1 of bulk carriers*, 2003, Marine Structures 16, pp. 601–626;

[18] **Tveiten BW, Moan T.,** *Determination of structural stress for fatigue assessment of welded aluminum ship details,* Mar Struct 2000; 13(3), pp. 189–212.